



# Removal of antibiotic from aqueous solution using synthesized TiO<sub>2</sub> nanoparticles: characteristics and mechanisms

Thi Huong Dao<sup>1</sup> · Thi Thuy Tran<sup>1</sup> · Van Ri Nguyen<sup>1</sup> · Thi Ngoc Mai Pham<sup>1</sup> · Cuong Manh Vu<sup>2,3</sup> · Tien Duc Pham<sup>1</sup> 

Received: 6 January 2018 / Accepted: 6 May 2018 / Published online: 11 May 2018  
© Springer-Verlag GmbH Germany, part of Springer Nature 2018

## Abstract

We investigated the removal of cefixime antibiotic (CEF) from aqueous solution using TiO<sub>2</sub> nanoparticles (TiO<sub>2</sub>-NPs) in the present study. The TiO<sub>2</sub>-NPs, which were successfully synthesized using sol–gel method, were characterized by X-ray diffraction, scanning electron microscopy and Fourier transformation infrared spectroscopy (FT-IR) techniques. The removal of CEF using synthesized TiO<sub>2</sub>-NPs as a photocatalyst with ultraviolet (UV) light was evaluated by the UV spectroscopic method. The optimum parameters for removal of CEF using TiO<sub>2</sub>-NPs such as contact time, pH of solution, initial concentration of CEF and dosage of TiO<sub>2</sub>-NPs were systematically studied and found to be 90 min, 6.0, 80 ppm and 0.1 mg/mL, respectively. The degradation efficiency of about 90% was achieved under the optimum conditions. Experimental kinetic results, which were fitted by the pseudo-second-order model, were much better than with pseudo-first order. The changes in surface charge of TiO<sub>2</sub>-NPs and surface functional groups were evaluated by zeta potential measurements and FT-IR, respectively. Based on UV spectroscopy, FT-IR spectroscopy and zeta potential measurements, we demonstrate that the removal mechanism of CEF is photocatalytic degradation by TiO<sub>2</sub>-NPs catalysis than adsorption of CEF onto TiO<sub>2</sub>.

**Keywords** Photocatalytic degradation · Adsorption · TiO<sub>2</sub> nanoparticle · FT-IR · Cefixime

## Introduction

Since the last two decades, intensive antibiotics for human, veterinary and agricultural purposes have increased rapidly (Díaz-Cruz et al. 2003; Hirsch et al. 1999; Kümmerer 2009; Le Corre et al. 2012). Cefixime (CEF) belongs to the third generation of beta lactam antibiotics that are widely used in many daily activities. The consumers of CEF rise significantly by the effective against susceptible bacteria since the injection of the middle ear, urinary tract infections, gonorrhea while some respiratory illnesses such as

pneumonia, bronchitis, laryngitis have also increased (Golcu et al. 2005; Jain et al. 2010). CEF is a primary candidate for switch therapy owing to its good efficiency and safety profile. CEF is used as the most convenient solution, because it is safe, effective and cheap to treat many diseases. However, the presence of a high concentration of antibiotics in the natural environment has been associated with the toxicity and the prevalence of resistance to antibiotics and bacterial species increase (Kitamura et al. 1990; Magit et al. 1994; Schwartz et al. 2003). The residual CEF eliminated into the water environment can cause serious pollution.

Many researchers have investigated the treatment methods to remove organic pollutants from the water environment (Ayodele 2013; Grčić et al. 2012; Klauson et al. 2010). The techniques are based on biological processes, chemical processes, physical processes or a combination of some of them (Ayodele 2013; Fakhri and Adami 2014; Guo and Chen 2015; Michael et al. 2013). The processes have been used for removing pollutants from aqueous solution such as membrane process, ozonation (Akmehmet Balcioğlu and Ötger 2003), fenton oxidation (Karthikeyan et al. 2012), adsorption (Gupta et al. 2005, 2009, 2013; Gupta and Nayak 2012; Mittal et al. 2009;

✉ Cuong Manh Vu  
vumanhcuong309@gmail.com

✉ Tien Duc Pham  
tienduchphn@gmail.com; tienducpham@hus.edu.vn

<sup>1</sup> Faculty of Chemistry, VNU University of Science, Vietnam National University-Hanoi, 19 Le Thanh Tong, Hoan Kiem, Hanoi 10000, Vietnam

<sup>2</sup> Center for Advanced Chemistry, Institute of Research and Development, Duy Tan University, Da Nang, Vietnam

<sup>3</sup> Chemical Department, Le Quy Don Technical University, 236 Hoang Quoc Viet, Hanoi, Vietnam

Pham et al. 2014, 2015a, b, 2017a, b, 2018; Saleh and Gupta 2014; Zare et al. 2016) and photocatalytic degradation using ultraviolet–visible (UV–Vis) irradiation (Gupta et al. 2011, 2012; Saravanan et al. 2013a, c, 2015b, 2016, d). Among them, photocatalytic degradation is one of the most effective techniques for treating residual pharmaceutical products in water and wastewater (Fang et al. 2011; Gupta et al. 2012; Herrmann et al. 1993; Santiago-Morales et al. 2013; Sousa et al. 2013). This method can apply to remove both organic and inorganic pollutants. Guo and Chen (Guo and Chen 2015) investigated the removal of cephalosporins using alga-activated sludge, while the group of Pourtaheri studied photocatalytic degradation of CEF using incorporated NiO onto clinoptilolite nanoparticles (Pourtaheri and Nezamzadeh-Ejhih 2015). Although the authors focused on the removal of CEF, various complicated pretreatment steps were required. For developing countries, a simple and high efficiency for treating CEF is preferable. Nevertheless, no studies regarding the release of CEF from aqueous solution using TiO<sub>2</sub> nanoparticles (TiO<sub>2</sub>-NPs) have been reported. The TiO<sub>2</sub>-NPs have high specific surface area so that adsorption of CEF on the TiO<sub>2</sub> surface can occur. The confirmation of removal of CEF using TiO<sub>2</sub>-NPs by photocatalytic degradation or adsorption has not been published.

The synthesized procedure of TiO<sub>2</sub>-NPs is also important because it highly influences the removal efficiency of CEF. The preparation of TiO<sub>2</sub>-NPs can be conducted by various methods, such as vapor deposition, solvothermal, electrochemical, micelle and inverse micelle, combustion flame-chemical vapor condensation, plasma evaporation and sol–gel (Grčić et al. 2012; Joseph et al. 2008; Pourtaheri and Nezamzadeh-Ejhih 2015; Praveena et al. 2011; Shojaie and Loghmani 2010; Song et al. 2011).

In the present study, we used the sol–gel method because it is one of the simplest techniques to synthesize TiO<sub>2</sub>-NPs. The effective conditions for fabrication of TiO<sub>2</sub>-NPs including initial concentration, pH of solvent and calcination time were studied. Characterizations of TiO<sub>2</sub>-NPs were examined by X-ray diffraction (XRD), scanning electron microscopy (SEM), transform infrared spectroscopy (FT-IR) and zeta potential measurements. For determining CEF concentrations, UV–Vis spectroscopy method was used due to its convenience, simplicity, ease of use and being inexpensive (Attimarad et al. 2012; Kandhro et al. 2013; Kitamura et al. 1990; Magit et al. 1994; Mallick et al. 2008; Midtvedt 2008; Pourtaheri and Nezamzadeh-Ejhih 2015). To our best knowledge, this is the first systematic report regarding the removal of CEF from aqueous solutions using synthesized TiO<sub>2</sub>-NPs. We also investigate the optimum conditions for treating CEF such as contact time, pH of solution and dosage of TiO<sub>2</sub>-NPs. The degradation mechanisms of CEF using

TiO<sub>2</sub> nanoparticles are also proposed based on UV–Vis, FT-IR and zeta potential measurements.

## Experimental

### Materials and chemicals

Vietnam National Institute of Drug Quality Control supplied an Asian standard of cefixime, CEF (C<sub>16</sub>H<sub>15</sub>N<sub>2</sub>O<sub>7</sub>S<sub>2</sub>), with purity higher than 99%. The chemical structure of CEF is indicated in Fig. 1.

Organic solvents such as methanol and ethanol with analytical grade were purchased from Scharlau (Spain). The stock solution of 1000 ppm CEF was prepared and kept in a dark bottle in a refrigerator at 8 °C for 1 week. Tetrabutylorthotitanate (TBOT) (C<sub>16</sub>H<sub>36</sub>O<sub>4</sub>Ti, Merck, Germany) was used to synthesize TiO<sub>2</sub>-NPs. Phosphoric acid, boric acid, sodium acetate, ammoniac and ammonium chloride, of analytical grade (Merck), were used to prepare the buffer solution from pH 2 to pH 10. Other chemicals were purchased from Merck with analytical grade. A UV-C lamp with wavelength from 280 to 100 nm (Ballast) was used in the photoreactor in the photocatalytic degradation process. Ultrapure water system (Labconco, USA) with resistivity 18.2 MΩ.cm was used to produce ultrapure water in preparing solutions and in all measurements.

### Preparation of TiO<sub>2</sub> nanoparticles

We used the procedure described by Wu and coworkers (Wu et al. 2005) to synthesize TiO<sub>2</sub>-NPs in the present study. Firstly, a solution of 70 mL of ethanol was put in a beaker, and then 35 ml of TBOT with 0.46 mL concentrated nitric acid was added to form an oxidation inhibitor (A solution). This solution was thoroughly stirred to make a sol. Another 70 mL ethanol with was mixed well with 10 mL ultrapure water (B solution). After that, the solution was continuously stirred for 40 min and then we added the B solution into A

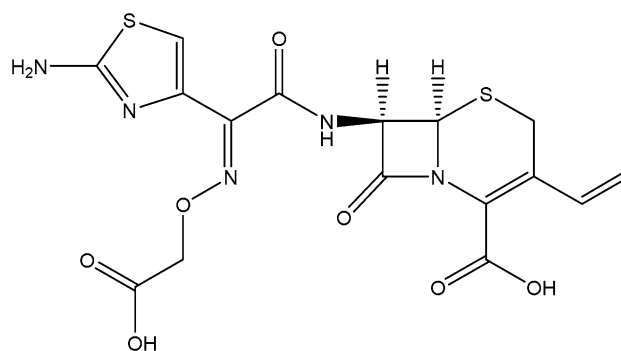


Fig. 1 The chemical structure of cefixime (CEF)

solution with stirring until the sol became a gel. Secondly, the gel was dried in a drying cabinet at 95 °C for 24 h. In the next step, we ground the dry gel to a powder. Finally, the powder was calcined at 500 °C for 2 h before cooling to room temperature in a desiccator. Finally, the powder was well grinded to form nanosized TiO<sub>2</sub>. The schematic representation of the fabricated procedure of TiO<sub>2</sub>-NPs is described in Fig. 2.

**Photocatalytic degradation experiments**

Photocatalytic degradation experiments were performed in a cylindrical laboratory batch reactor. Novel reactor configurations with a volume of 100 mL contained the sample and a magnetic stirrer in the presence of Ballast UV-C light with the primary emission output under a wavelength of 280 nm used as the source of UV-C irradiation. The photoreactor is schematically represented in Fig. 3. The sample was put in a glass cylindrical vessel enclosed by a silver shell to avoid the UV radiation effect on the human body. The cooling bath was used to keep the temperature constant at all conditions. The stirring bar was continuously worked to disperse TiO<sub>2</sub>-NPs in the solution.

Photocatalytic degradation was conducted with different conditions of CEF concentration from pH 2 to pH 10. The examined concentrations of CEF in the order of 15, 25, 40 and 50 ppm were prepared from stock solution. The

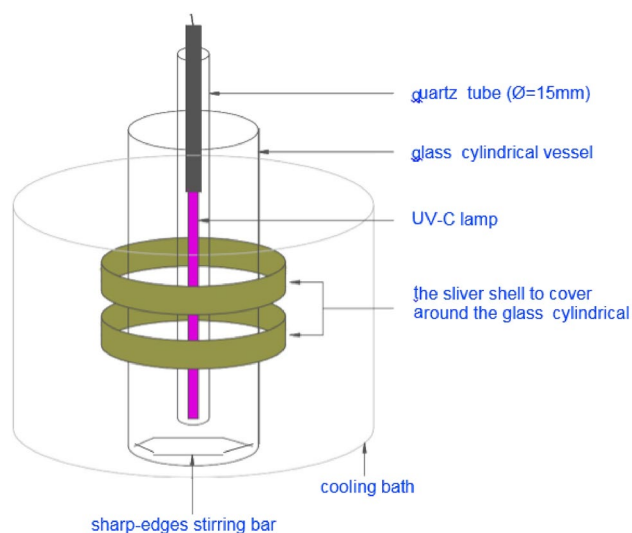


**Fig. 3** Schematic and geometric characteristics of the laboratory batch reactor (CBPR)

contact time was in the range of 15–120 min. The effect of TiO<sub>2</sub>-NPs dosage was studied at the concentrations of 0.0010, 0.0100, 0.1000 and 1.0000 mg/mL. The reaction temperature was kept constant at 24 ± 1 °C by using a photoreactor. All experiments were carried out three times at atmospheric pressure.

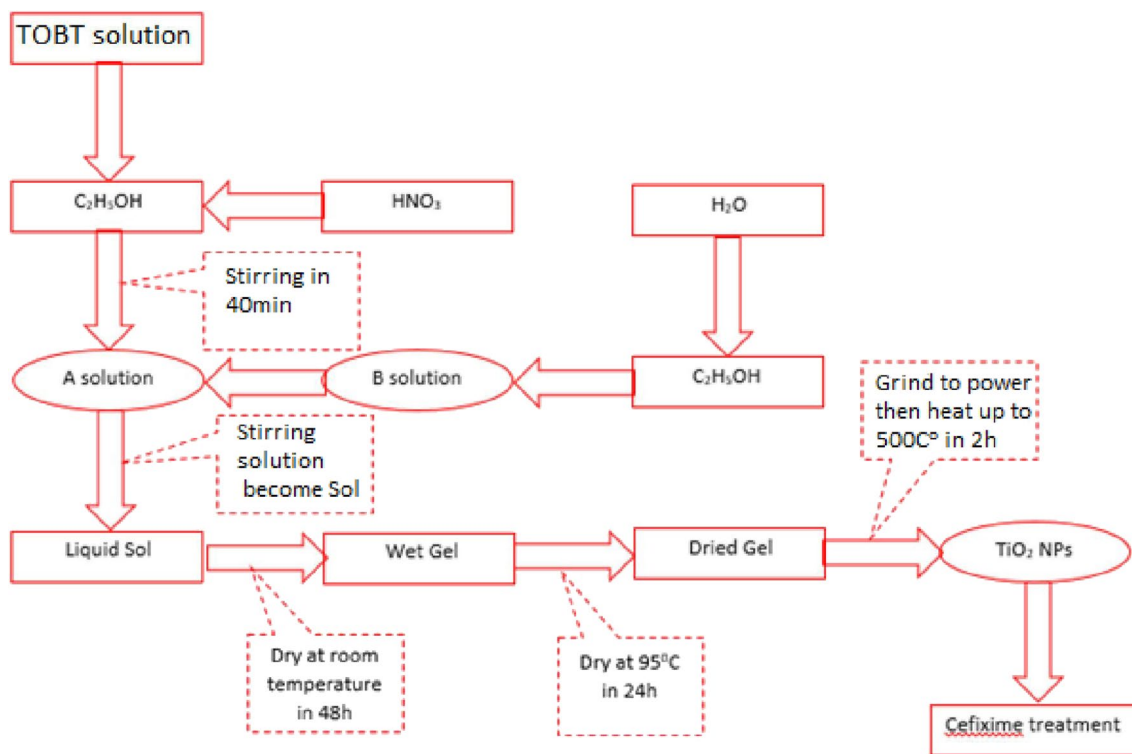


**Fig. 2** Schematic synthesizing process of TiO<sub>2</sub> nanoparticles

## Spectroscopic method

The concentrations of CEF were analyzed by the spectroscopic method using a UV–Vis spectrophotometer (UV-1650PC, Shimadzu, Japan) with quartz cuvettes of 1 cm optical path length.

The degradation efficiency of CEF was examined by the difference of concentration of CEF in aqueous solution before and after removal. The degradation efficiency of CEF (%  $D$ ) was calculated using the following equation:

$$\%D = (C_i - C_t) \times 100 / C_i, \quad (1)$$

where  $D$  is the degradation efficiency, and  $C_i$  and  $C_t$  are the initial CEF concentrations and concentrations of CEF at the time  $t$ , respectively.

## Characterization of TiO<sub>2</sub> nanoparticles

X-ray diffraction (XRD) was obtained on a Bruker D8 Advance X-ray diffractometer with CuK<sub>α</sub> radiation ( $\lambda = 1.5418 \text{ \AA}$ ). The intensity of the diffraction peaks was recorded in the 20–700 ( $2\theta$ ) range with a step size of 0.03°.

The crystal structure of the TiO<sub>2</sub>-NPs can be determined by power X-ray diffraction (XRD). The average size of nanoparticle was calculated by the Scherer's equation (Patterson 1939):

$$D = \frac{K\lambda}{\beta \cos \theta}, \quad (2)$$

where  $D$  is the average crystallite sizes of anatase or rutile,  $K$  (0.94) is a shape factor, the wavelength of Cu K<sub>α</sub> radiation is ( $\lambda = 0.1542 \text{ nm}$ ),  $\beta$  is the full-width at half-maximum (FWHM) of the main intensity peak, and  $\theta$  is the angle of diffraction.

The morphology of synthesized TiO<sub>2</sub>-NPs was examined by scanning electron microscopy (SEM, HITACHI S4800, Japan).

To evaluate the functional groups of CEF and surface modification of TiO<sub>2</sub>-NPs before and after treating CEF, Fourier transform infrared (FT-IR) spectroscopy was performed. The infrared spectra were obtained by an FT-IR spectrometer (Affinity-1S, Shimadzu, Japan). All recorded spectra were obtained at 25 °C and atmospheric pressure at a resolution of 4 cm<sup>-1</sup>.

The charging behavior of TiO<sub>2</sub> nanoparticles with and without degradation of CEF was examined using a Zeta phoremeter IV (CAD Instrumentation) at a temperature of 25 °C, pH = 6 and with a background electrolyte of 1 mM.

The  $\zeta$  potential was calculated from electrophoretic mobility using Smoluchowski's equation (HS) (Delgado et al. 2007):

$$\zeta = \frac{u_e \eta}{\epsilon_{rs} \epsilon_0}, \quad (3)$$

where  $\zeta$  is the zeta potential (mV),  $u_e$  is the electrophoretic mobility ( $\mu\text{ms}^{-1}/\text{Vcm}^{-1}$ ),  $\eta$  the dynamic viscosity of the liquid (mPa s),  $\epsilon_{rs}$  the relative permittivity constant of the electrolyte solution and  $\epsilon_0$  is the electric permittivity of the vacuum ( $8.854 \times 10^{-12} \text{ F/m}$ ).

## Results and discussion

### Analytical method

The concentrations of CEF in all measurements were determined by UV spectroscopy. The spectra of 25 ppm CEF in aqueous solution are indicated in Fig. 4. As can be seen in Fig. 4, the spectrum has only one peak at 288.0 nm that is characterized for CEF. The spectrum of CEF agrees well with previous studies (Attimarad et al. 2012).

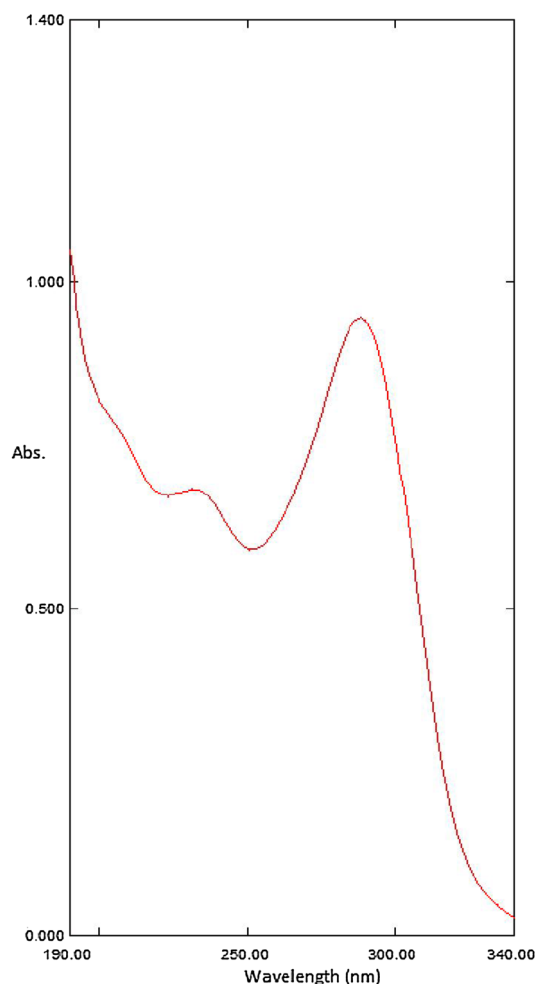


**Fig. 4** UV spectrum of cefixime with a concentration of 25 ppm has maximum absorbance (Abs) at a wavelength of 288 nm

## Characterizations of TiO<sub>2</sub> nanoparticles

The characterizations of TiO<sub>2</sub>-NPs were examined by X-ray diffraction (XRD) and scanning electron microscopy (SEM). In Fig. 5, the large peaks which occurred at  $2\theta = 25.265^\circ$  were observed in the XRD pattern of synthesized TiO<sub>2</sub>-NPs. Khataee and coworkers (Daneshvar et al. 2004, 2006, 2005; Khataee and Kasiri 2010) indicated that the TiO<sub>2</sub> anatase phase had peaks at  $\theta = 12.65^\circ$ ,  $18.90^\circ$  and  $24.054^\circ$ , while the rutile one was found at  $\theta = 13.75^\circ$ ,  $18.10^\circ$  and  $27.20^\circ$ . The appeared peaks of synthesized TiO<sub>2</sub>-NPs in the present study were encountered at  $\theta = 12.65^\circ$ ,  $12.85^\circ$ ,  $15.40^\circ$  and  $18.10^\circ$ . Therefore, the XRD pattern confirms that the main morphology of TiO<sub>2</sub> in our case is the anatase phase. In addition, we can calculate the mean particle sizes of TiO<sub>2</sub> using Scherer's equation (Eq. 2). The average diameter of particles was found to be  $26 \pm 5$  nm.

The surface morphology of TiO<sub>2</sub>-NPs was examined by SEM (Fig. 6). The SEM images of TiO<sub>2</sub>-NPs were obtained with the resolutions of 400 nm (a) and 200 nm (b). As can be seen in Fig. 6, the particles agglomerated into bundles of flaky spherical morphology. The nanosized TiO<sub>2</sub> can induce a large specific surface area that is good for photocatalytic degradation and adsorptive removal of CEF with TiO<sub>2</sub>-NPs. It implies that the size of TiO<sub>2</sub> particles is important for the degradation efficiency of CEF in solution. For photocatalytic degradation of CEF, TiO<sub>2</sub> illuminated  $\lambda \leq 390$  nm light electrons are excited out of their energy level and consequently leave a hole in the valence band to give the OH<sup>•</sup> radicals, which are powerful oxidizing agents. These may attack the CEF molecules near the surface of TiO<sub>2</sub> (Daneshvar et al. 2006). For adsorption of CEF on TiO<sub>2</sub>-NPs, larger specific area induces a higher number of sites of adsorbent. Thus, adsorption may induce the removal of CEF by TiO<sub>2</sub>-NPs.

## Degradation studies

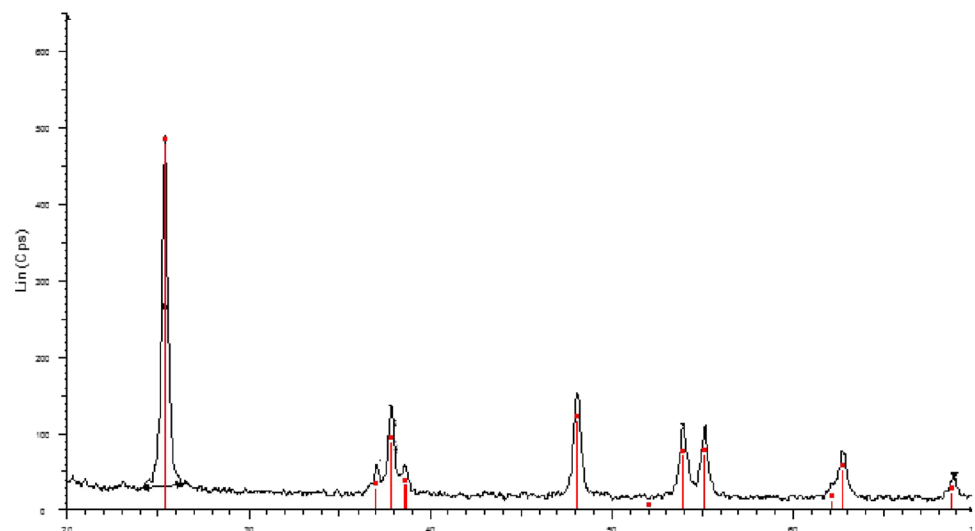
### Effect of time

The effect of time was carried out with a solution containing of 15 ppm CEF in the presence of 0.10 mg/mL TiO<sub>2</sub> under UV light. 10.0 mL of samples was taken and then centrifuged with a high speed of 15,000 rpm for 30 min to eliminate TiO<sub>2</sub>-NPs in the solution. Then, the collected solutions were examined by UV spectroscopy. The degradation of CEF as a function of contact time is indicated in Fig. 7. As can be seen in Fig. 7, the degradation efficiency of CEF increased with increase in time. The maximum degradation efficiency which was about 90%, was achieved after 90 min. This result suggests that the required time for the degradation process is 90 min. Figure 7a also shows that at the first step, the degradation achieved with the higher efficiency than that at 45 min later due to the decomposition of CEF molecular affecting by photocatalyst of TiO<sub>2</sub>-NPs. In Fig. 7b, the absorbance of CEF decreased rapidly after 15 min. The attraction of CEF molecules to the TiO<sub>2</sub> surface can induce the reaction that occurs steadily initially than at the final process. This can be explained following the reactions shown by Daneshvar et al. (Daneshvar et al. 2003). The lifetime of OH<sup>•</sup> was not so long that it could not react with the nearby CEF molecules.

### Effect of pH

The pH of the solution plays an important role in the degradation of CEF by TiO<sub>2</sub>-NPs because it can influence the surface charge, effective catalysis of TiO<sub>2</sub> and charging behavior of CEF. The effect of pH on the degradation of CEF was conducted in the pH range 2–10 (Fig. 8a). The degradation efficiency of CEF increased from pH 2 to pH 6 and then

**Fig. 5** X-ray pattern of synthesized TiO<sub>2</sub> nanoparticles



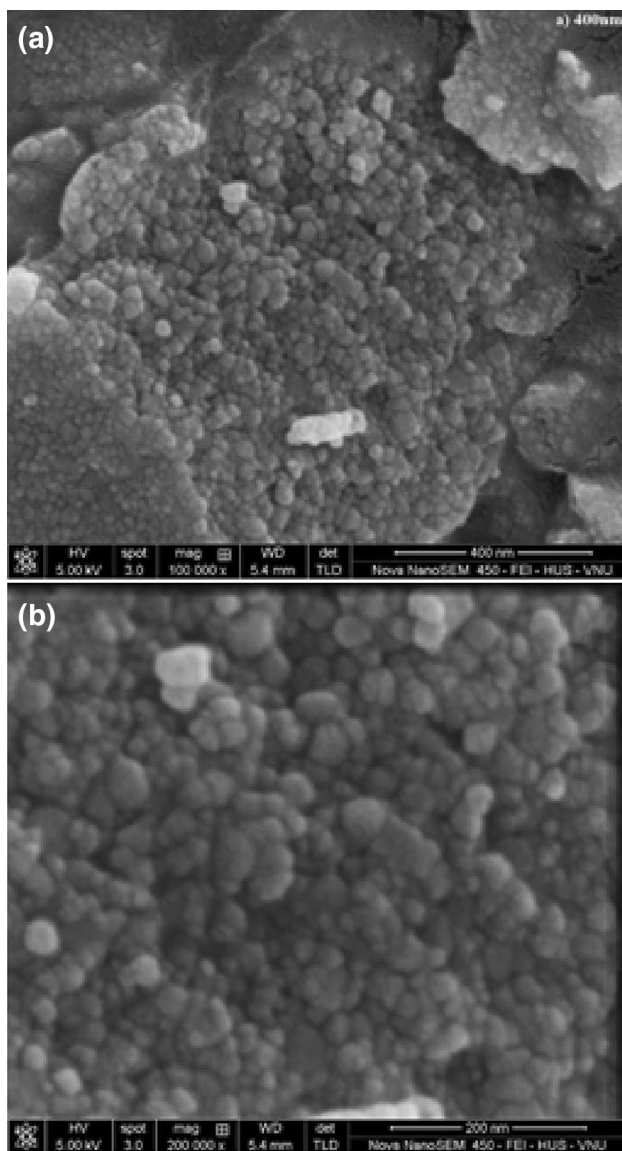


**Fig. 6** SEM images of  $\text{TiO}_2$  nanoparticles with different scales. **a** 400 nm and **b** 200 nm

decreased from pH 6 to pH 10. The standard deviations of three replicates at pH 6 are also small, indicating that the experiments have good repetitiveness. Thus, the optimum pH was 6 in which a degradation efficiency of about 90% was achieved. According to the previous paper (Pourtaheri and Nezamzadeh-Ejhih 2015), the authors studied a heterogeneous photocatalyst using NiO nano-clinoptilolite (0.25 mg/mL of 13.3% NiO) under irradiation from an Hg-lamp for 250 min. The degradation efficiency of CEF was obtained under 80%. In the present work, the degradation efficiency reached up to 90%, while the required time was only 90 min. It demonstrates that the  $\text{TiO}_2$  here is effective material for removal of CEF compared with NiO. Other materials such as ZnO nanoparticles, ZnO–CdO, ZnO– $\text{V}_2\text{O}_5$

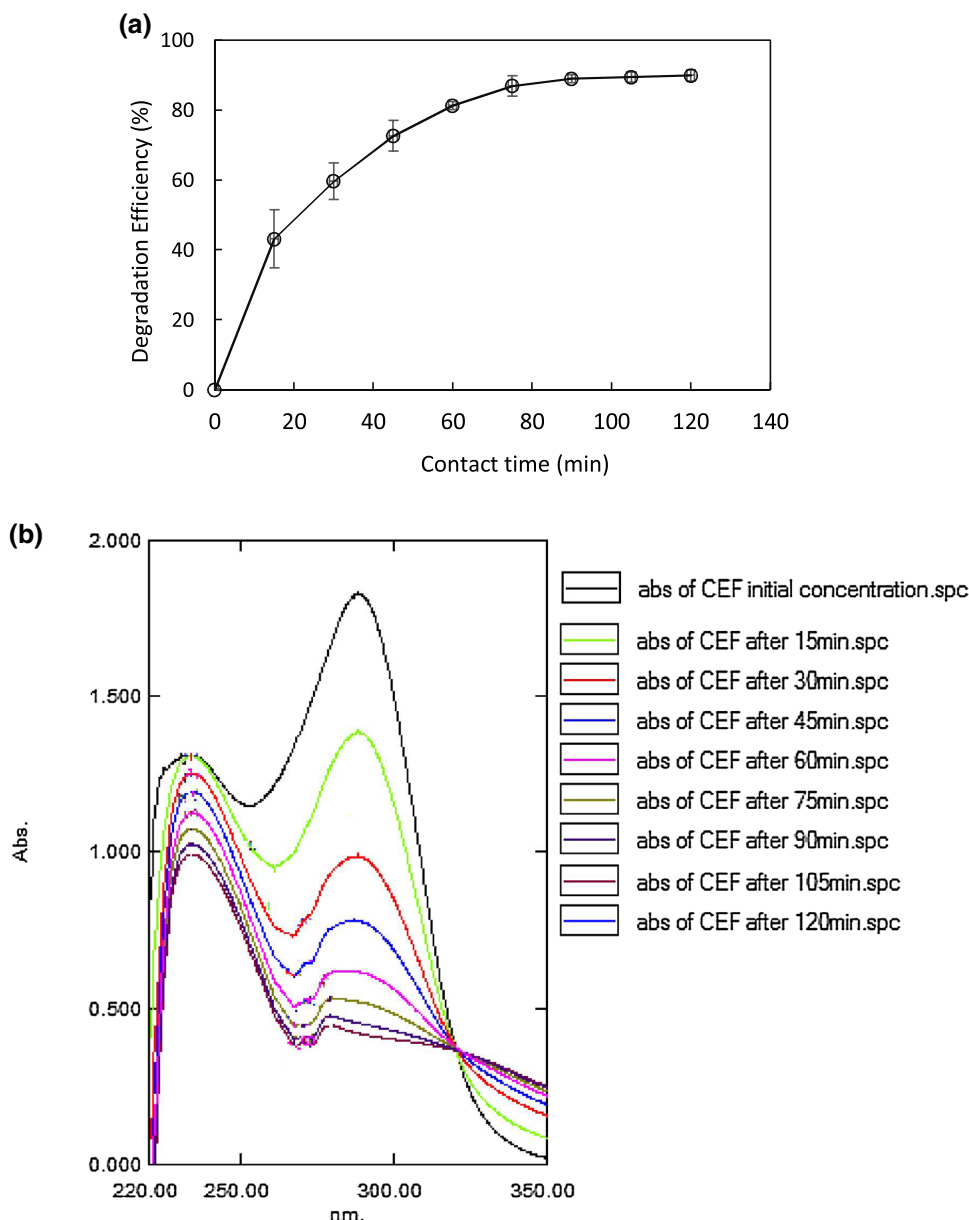
or ZnO–Ag nanocomposite were used in photocatalysis to remove organic contaminants, but the degradation efficiencies were not so high (Arun Jose et al. 2012; Saravanan et al. 2013a, b, c, 2015a, b, 2016). Although  $\text{TiO}_2$ -NPs is not a very cheap material, it seems to be a novel one for the removal of antibiotics from aqueous solution. The degradation efficiency of CEF was also studied following the time with different pH values of 3, 6 and 9 under UV light for 90 min (Fig. 8b). The degradation efficiency of CEF at pH 6 is always higher than that at pH 3 and at pH 9. It suggests that pH significantly affects the stability of CEF and the activity of  $\text{TiO}_2$  catalyst.

Let us discuss the effect of pH on the efficiency of degradation processes in more detail. Titania has an amphoteric behavior, so that the change in surface charge of  $\text{TiO}_2$  is strongly dependent on pH. When the pH of the solution is toward neutral condition, the valence band  $h\nu_{\text{VB}}^+$  can react with water to produce not only the hydroxyl radical, but also the proton can break the stable structure of CEF, since the structure of CEF at lower pH is in symmetrical balance which is more stable than the CEF structure in a neutral solvent (Hoffmann et al. 2012). Thus, CEF can be easily removed with a neutral pH solvent. It should be noted that the  $\text{TiO}_2$  is less reactive in acidic solvent. After absorbing UV light,  $\text{TiO}_2$  can produce the  $\text{OH}^-$  radical in alkaline solution and then both  $\text{OH}^-$  radical and  $\text{H}^+$  are formed inducing a neutral solution (Daneshvar et al. 2006). Therefore, the optimum pH for degradation of CEF under UV/  $\text{TiO}_2$  catalysis is pH 6.

### The effect of $\text{TiO}_2$ dosage

The dosage has a significant effect on the degradation process, because it can influence the total specific surface area of particles and the number of binding sites (Pham et al. 2017a). The tests were taken at different amounts of catalyst. Figure 9 indicates that the degradation efficiency was lowest when using  $\text{TiO}_2$ -NPs without UV light. On the other hand, the degradation efficiency increases with an increase of  $\text{TiO}_2$  dosage from 0.001 to 10 mg/mL (Fig. 9). The optimum dosage of  $\text{TiO}_2$  was 0.1 mg/mL, while the degradation efficiency was found to be about 90%. When the dosage increased higher than 0.1 mg/mL, the degradation efficiency decreased due to the fast flocculation at high concentration of  $\text{TiO}_2$ -NPs. Furthermore, with an increase of the dosage of catalyst, the opacity of the suspension increases, as a result of excess of  $\text{TiO}_2$  particles (Gonçalves et al. 1999). When the reaction occurs under only UV light, the removal of CEF decreases only under 50% after 90 min. These results show that CEF can decompose by itself under light, but it is much slower than that in the presence of  $\text{TiO}_2$ -NPs. The removal of CEF reported in the reference (Pourtaheri and Nezamzadeh-Ejhih 2015) is nearly 50% for 90 min. However, when

**Fig. 7** The degradation efficiency of CEF using TiO<sub>2</sub>-NPs as a function of time. **a** The degradation efficiency changes from 0 to 150 min. Error bars show the standard deviations of three replicates. **b** The spectra of CEF from 220 to 350 nm as a function of time with the initial concentration of 20 ppm



using TiO<sub>2</sub>-NPs, the removal of CEF can increase up to 90% with the dosage of catalysis 0.1 mg/mL (concentration of CEF is 25 ppm). Therefore, the optimum TiO<sub>2</sub> dosage is 0.1 mg/mL and it is fixed for further studies.

**The effect of initial cefixime concentration**

The initial concentration of CEF was examined with different concentrations of 10, 20, 40, 50, 60 and 80 ppm in the presence of 0.1 mg/mL of TiO<sub>2</sub>-NPs under UV-C irradiation. As can be seen in Fig. 10, when increasing the initial concentration of CEF, the final CEF concentration decreases with increasing concentration, except for the initial concentration of 10 ppm. Figure 10 shows that the degradation strongly depends on the initial concentration of CEF. In other words,

the initial CEF concentration has a pronounced effect on the degradation rate. The results demonstrate that conversions are less in the solution with higher initial concentration compared with the conversion in the lower concentration solution. It can be explained by the decrease in the number of activated sites on the TiO<sub>2</sub> surface due to the conversion of the surface with CEF molecules, which is proportional to the initial concentration of CEF (Daneshvar et al. 2004). On the basis of the above considerations, photocatalytic reaction can account for the reaction between the CEF molecules and the hydroxyl radical over the catalyst surface. At the lowest concentration (10 ppm), the CEF shows less performance in reacting with the radicals so that the degradation efficiency is not high. In addition, when the concentration of the catalyst increased up to 80 ppm, the performance of the

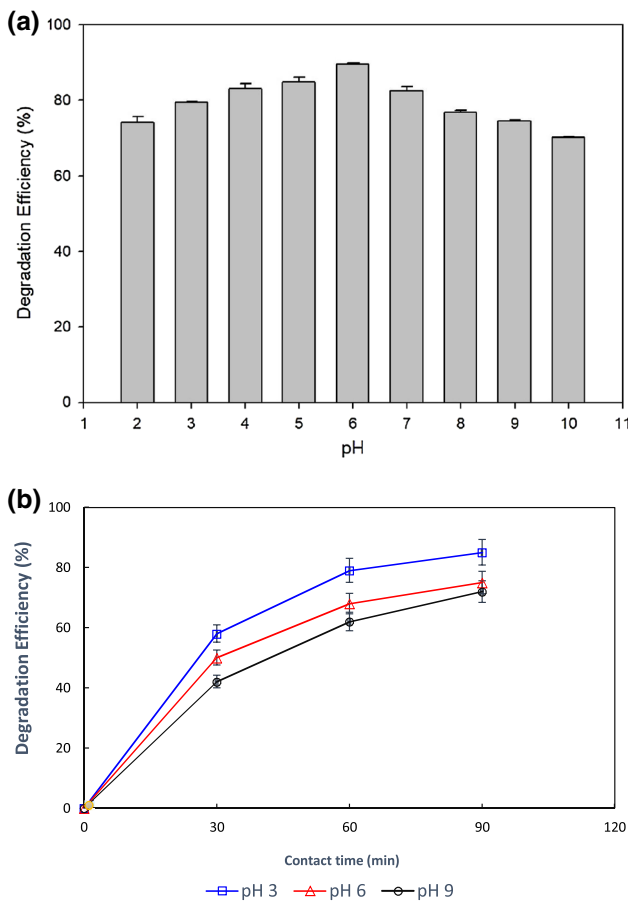


**Fig. 8** The change in the degradation efficiency of cefixime in the presence of 0.1000 g/L TiO<sub>2</sub>-NPs **a** at different pH values from 2 to 10; **b** by following time at pH 3, pH 6 and pH 9. Error bars show the standard deviations of three replicates

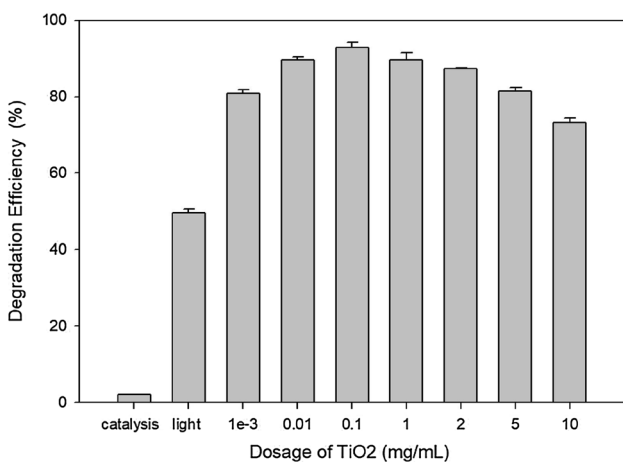


**Fig. 9** The role of some parameters and TiO<sub>2</sub> dosage of the photo-degradation process. Error bars show the standard deviations of three replicates

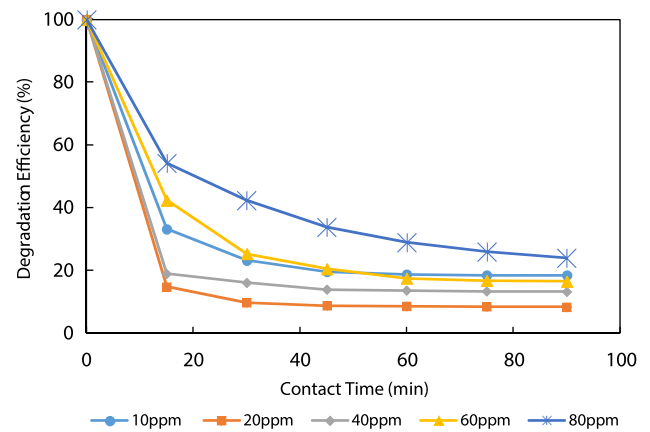


**Fig. 10** The change in the degradation efficiency of CEF with different initial concentrations

catalyst fell into an “overload” state, in which the production of catalyst radicals was not enough for the react with the CEF molecules. As a result, it could reduce the effectiveness of the treatment process, which is in good agreement with the results of the concentration declining to about 20 ppm.

### Kinetic studies of the photodegradation process

The kinetics of photodegradation of antibiotic using TiO<sub>2</sub>-NPs was studied with different initial concentrations of CEF. We tried to fit experimental data using the first- and second-pseudo-order models.

The first-pseudo-order model equation is:

$$R = -\frac{dA}{dt} = K C, \tag{4}$$

$$\ln C_t = \ln C_o - kt, \tag{5}$$

where  $C_t$  and  $C_o$  are the concentration at the time  $t$  and the initial concentration respectively, and  $k$  is the reaction constant.

This model has been applied in the CEF degradation process, used to study the kinetics of CEF degradation. The results shown in Fig. 11 do not have a good correlation coefficient. Thus, the degradation kinetics did not follow the first-order model.

The pseudo-second-order equations are:

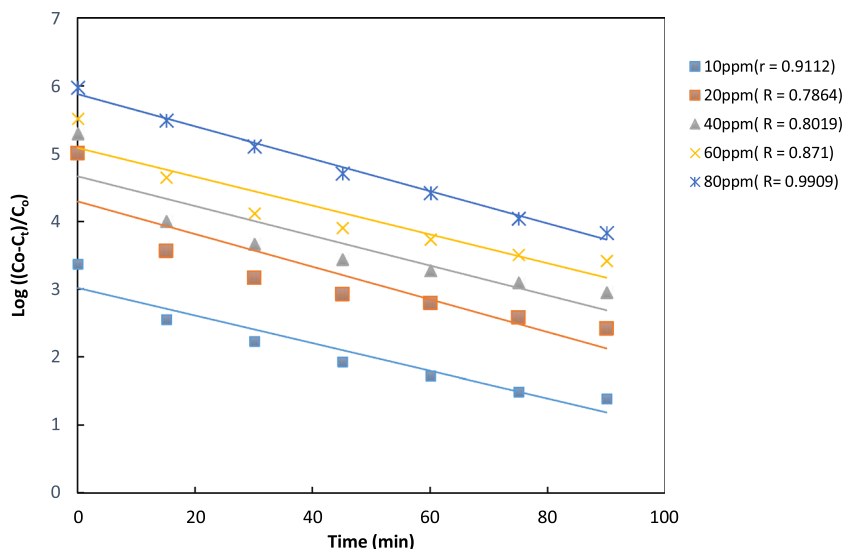
$$R = k \frac{KC}{1 + KC_i} = K_{obs} C, \tag{6}$$

$$\frac{1}{K_{obs}} = \frac{1}{kk'} + \frac{C_i}{k}, \tag{7}$$

where  $C_i$  is the initial concentration,  $C$  is a constant,  $K$  is the Langmuir–Hinshelwood adsorption equilibrium constant (ppm<sup>-1</sup>),  $K_{obs}$  is the pseudo-second-order rate constant



**Fig. 11** The kinetics of CEF photodegradation calculated by the first-order model



( $\text{min}^{-1}$ ), and  $k, k'$  are the reaction rate constant of the forward and conversion reaction, respectively.

Figure 12 shows that the second-pseudo-order model can fit the kinetic data well with the correlation coefficient higher than 0.98, while initial concentration of CEF ranges from 10 to 60 ppm. However, at the CEF concentration of 80 ppm, this kinetic model seems not to be very good. It suggests that in this case, the auxiliary mechanism such as the adsorption process can be induced at high CEF concentration.

The results in Figs. 11 and 12 show that the first-pseudo-order model has much lower correlation coefficient than the second-pseudo-order model. Therefore, the kinetic rate can be calculated based on the second-pseudo-order model.

The mechanisms for degradation of CEF are discussed in more detail based on the surface modification by FT-IR spectroscopy and zeta potential measurement as given below.

**Suggested mechanisms**

**The zeta potential measurements**

Electrophoretic mobility measurement is a useful technique to characterize the charging behavior of many materials (Huang et al. 2017; Kobayashi 2008; Pham et al. 2017a, 2018; Yamaguchi and Kobayashi 2016). The zeta potentials calculated from the electrophoretic mobility of  $\text{TiO}_2$ -NPs before and after photodegradation of CEF were obtained in a buffer solution at pH 6. Figure 13 shows that the mean of zeta potential of  $\text{TiO}_2$ -NPs is  $-34.99$  mV and it changes slightly to  $-37.79$  mV (examined at the same conditions) after CEF treatment.

At pH 6, CEF has negative charge so that the zeta potential of  $\text{TiO}_2$  with CEF decreases. If the adsorption induces the removal of CEF mainly, the zeta potential must be significantly changed. However, the decrease in zeta potential after CEF treatment is too small that adsorption is not the

**Fig. 12** The kinetics of CEF photodegradation calculated by the second-pseudo-order model

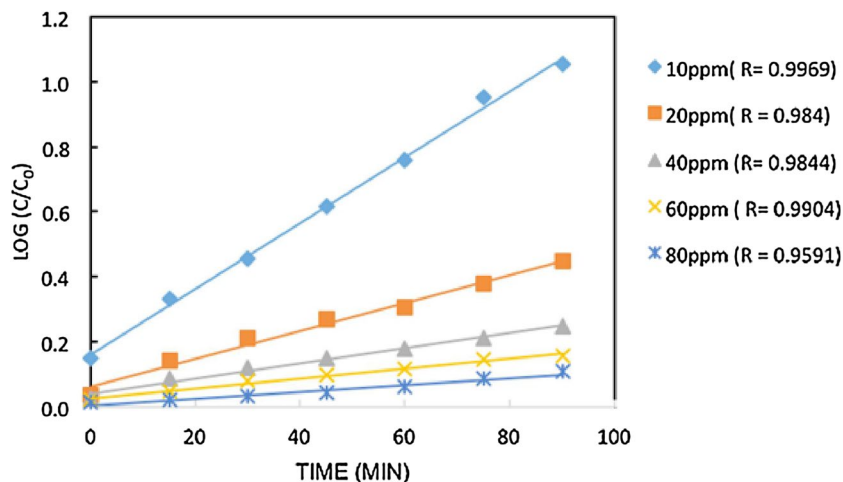
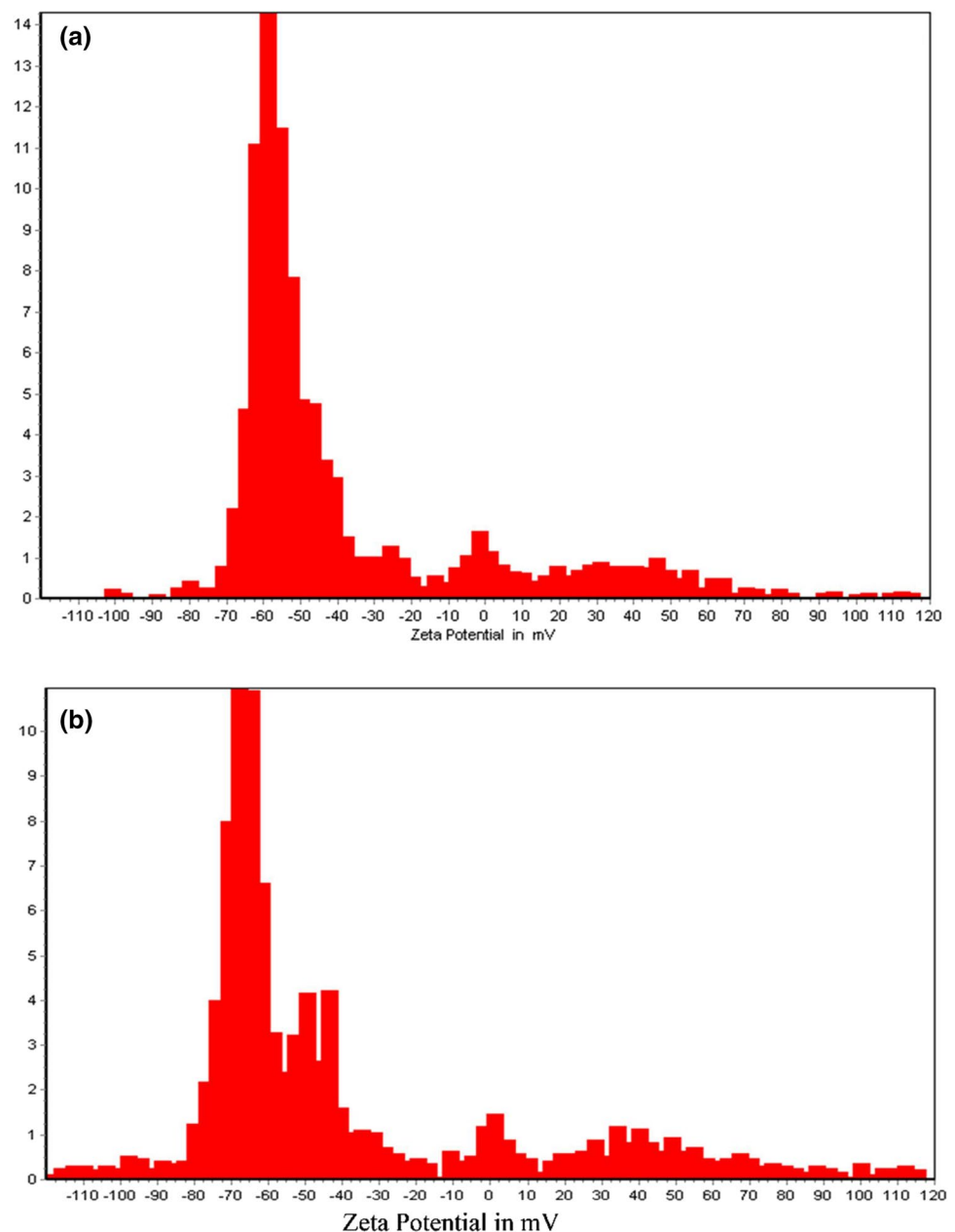


**Fig. 13** The distribution of zeta potential of  $\text{TiO}_2$  before CEF treatment (a) and after CEF treatment (b)



main process in this case. These results are in good agreement with previously published papers (Huang et al. 2017; Pham et al. 2018).

#### The change in the UV-Vis spectrum

Figure 14 shows the change in the UV spectrum of CEF after treatment. The characterization peak of CEF at 288 nm disappeared after using  $\text{TiO}_2$ -NPs and under UV-C light for 90 min. It should be noted that only using UV radiation for treating CEF, its concentration was decreased, but the spectrum still occurred (not indicated

here). The photocatalytic degradation process under UV light using  $\text{TiO}_2$ -NPs catalyst is also used to remove many organic compounds (Daneshvar et al. 2004, 2006). To study the mechanism, the surface active groups of  $\text{TiO}_2$  before and after CEF treatment were evaluated. The spectrum of CEF solution before treating using  $\text{TiO}_2$ -NPs was also conducted with the same conditions to compare with the spectrum of CEF solution after photodegradation. As can be seen in Fig. 14, the specific peak characterized for CEF at 288.0 nm disappeared after treatment, indicating that the photocatalytic degradation was completely achieved with very high efficiency.

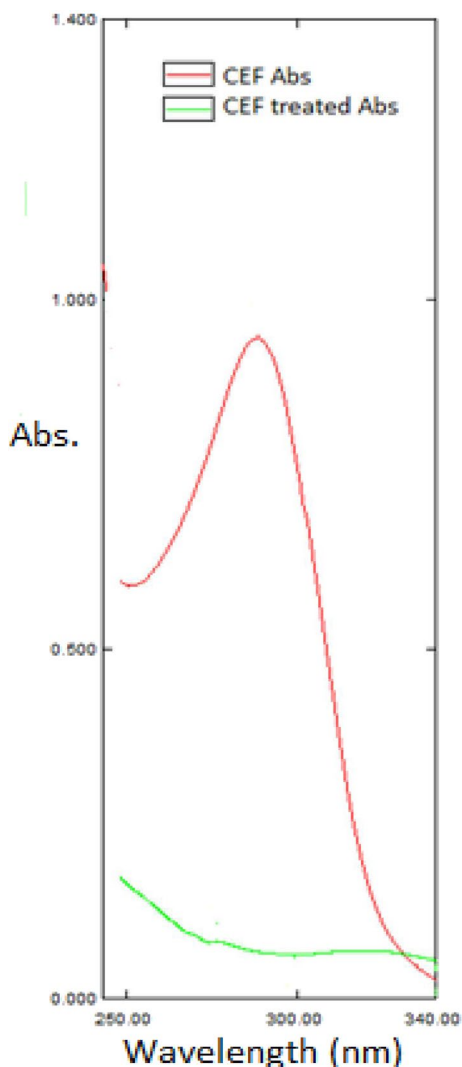


**Fig. 14** The spectrum of CEF after photodegradation under UV light and TiO<sub>2</sub> catalysis

**FT-IR spectra**

The Fourier transform infrared spectroscopy (FT-IR) is a useful tool to characterize functional groups for the removal of organic pollutants compared to the results of FT-IR of TiO<sub>2</sub> before and after treatment; however, the change in the spectra is not too great. In all the FT-IR spectra, a strong absorption band in the region 3000–3600 cm<sup>-1</sup> dominates. This band characterizes the OH-stretching vibrations of free and hydrogen-bonded surface hydroxyl groups. Water molecules can be strongly or weakly attached to the titanium surface forming a number of broad OH-stretching vibrations (inset in Figs. 15 and 16). The typical peaks of TiO<sub>2</sub> from 1200 to 1700 cm<sup>-1</sup> changed after treatment with CEF. In Fig. 15, we can see that some main peaks of the characterized groups of TiO<sub>2</sub> occurred at 1700 and 2300 cm<sup>-1</sup>, but

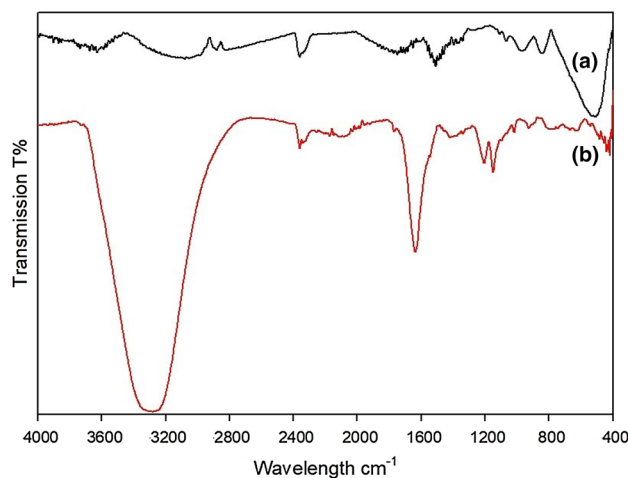


**Fig. 15** FT-IR spectra of TiO<sub>2</sub>-NPs **a** without CEF treatment and **b** after using for removal of CEF

after CEF treatment these peaks disappeared (in Fig. 15b). Based on this, the photodegradation process has changed the structure of TiO<sub>2</sub>. The results were examined again in comparison with the FT-IR spectra of CEF before treatment and after treatment (Fig. 16). A second typical absorption region of TiO<sub>2</sub> at 1200–1700 cm<sup>-1</sup> was reported and assigned to typically adsorbed water (H–O–H bending, peak at 1636 cm<sup>-1</sup>) and carbonate peaks at 1480 and 1410 cm<sup>-1</sup>. Prida et al. (Prida et al. 2007) indicated that the vibrations of carbonate interlayer ions in ternary hydroxalcite-like heyered double hydroxides occurred in the region of 870, 1360 and 640 cm<sup>-1</sup>. According to the results of FT-IR, the process

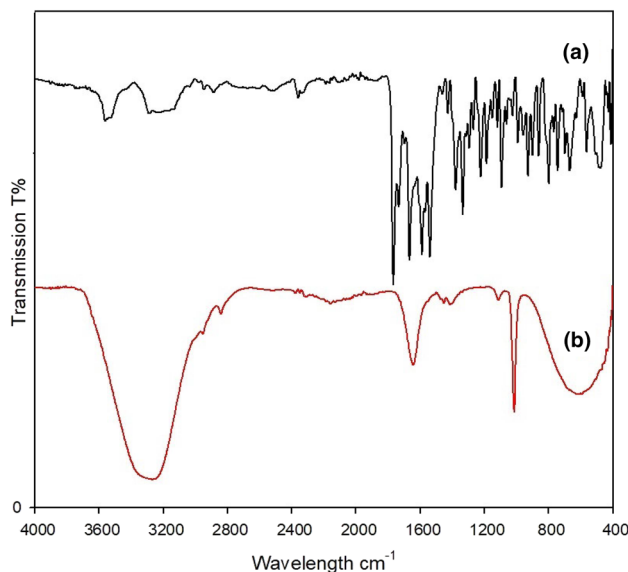


**Fig. 16** FT-IR spectrum of CEF **a** before treatment and **b** after treatment

mainly followed the photocatalytic mechanism, which is in good agreement with zeta potential measurements and the change in the UV spectrum.

## Conclusions

We have studied the degradation of cefixime antibiotic (CEF) using synthesized TiO<sub>2</sub> nanoparticles (TiO<sub>2</sub>-NPs) with UV-C irradiation light for the first time. The TiO<sub>2</sub>-NPs were successfully synthesized by the sol–gel method under operating conditions. The characteristics of TiO<sub>2</sub>-NPs were examined by the XRD, SEM and FT-IR methods. Some effective parameters on the photodegradation of CEF were optimized such as contact time 90 min, pH 6.0, dosage of TiO<sub>2</sub>-NP 0.1 mg/mL and initial concentration 80 ppm. The photodegradation kinetics followed a second-pseudo-order model than the first-pseudo-order model. Under optimum conditions, a degradation efficiency of about 90% was achieved, with initial concentration of CEF of 25 ppm. Due to the differences in the surface functional group before and after treatment by FT-IR, surface charge change by zeta potential measurement and degradation of CEF by UV spectroscopy, we suggested that the removal of CEF was mainly by photocatalytic degradation than adsorption. Our results indicate that photocatalytic degradation using TiO<sub>2</sub>-NPs is a novel material to remove beta lactam antibiotic from aqueous solution.

**Acknowledgements** This research is funded by Vietnam National Foundation for Science and Technology Development (NAFOSTED) under Grant Number 104.05-2016.17.

## Compliance with ethical standards

**Conflict of interest** The authors declare that they have no conflict of interest.

## References

- Akmehmet Balcioğlu I, Ötoker M (2003) Treatment of pharmaceutical wastewater containing antibiotics by O<sub>3</sub> and O<sub>3</sub>/H<sub>2</sub>O<sub>2</sub> processes *Chemosphere* 50:85–95. [https://doi.org/10.1016/S0045-6535\(02\)00534-9](https://doi.org/10.1016/S0045-6535(02)00534-9)
- Arun Jose L, Mary Linet J, Sivasubramanian V, Arora AK, Justin Raj C, Maiyalagan T, Jerome Das S (2012) Optical studies of nanostructured La-doped ZnO prepared by combustion method. *Mater Sci Semicond Process* 15:308–313. <https://doi.org/10.1016/j.mssp.2012.03.011>
- Attimarad M, Al-Dhubiab BE, Alhaider IA, Nair AB, Sree HN, Mueen AK (2012) Simultaneous determination of moxifloxacin and cefixime by first and ratio first derivative ultraviolet spectrophotometry. *Chem Cent J* 6:105–105. <https://doi.org/10.1186/1752-153x-6-105>
- Ayodele OB (2013) Effect of phosphoric acid treatment on kaolinite supported ferrioxalate catalyst for the degradation of amoxicillin

- in batch photo-Fenton process. *Appl Clay Sci* 72:74–83. <https://doi.org/10.1016/j.clay.2013.01.004>
- Daneshvar N, Salari D, Khataee AR (2003) Photocatalytic degradation of azo dye acid red 14 in water: investigation of the effect of operational parameters. *J Photochem Photobiol A* 157:111–116. [https://doi.org/10.1016/S1010-6030\(03\)00015-7](https://doi.org/10.1016/S1010-6030(03)00015-7)
- Daneshvar N, Hejazi MJ, Rangarany B, Khataee AR (2004) Photocatalytic Degradation of an organophosphorus pesticide phosalone in aqueous suspensions of titanium dioxide. *J Environ Sci Health B* 39:285–296. <https://doi.org/10.1081/pfc-120030242>
- Daneshvar N, Salari D, Niaei A, Rasoulifard MH, Khataee AR (2005) Immobilization of TiO<sub>2</sub> Nanopowder on glass beads for the photocatalytic decolorization of an azo dye C.I. Direct Red 23. *J Environ Sci Health A* 40:1605–1617. <https://doi.org/10.1081/ese-200060664>
- Daneshvar N, Salari D, Niaei A, Khataee AR (2006) Photocatalytic degradation of the herbicide erioglaucine in the presence of nanosized titanium dioxide: comparison and modeling of reaction kinetics. *J Environ Sci Health B* 41:1273–1290. <https://doi.org/10.1080/03601230600962302>
- Delgado AV, González-Caballero F, Hunter RJ, Koopal LK, Lyklema J (2007) Measurement and interpretation of electrokinetic phenomena. *J Colloid Interface Sci* 309:194–224
- Díaz-Cruz MS, López de Alda MAJ, Barceló D (2003) Environmental behavior and analysis of veterinary and human drugs in soils, sediments and sludge TrAc. *Trends Anal Chem* 22:340–351. [https://doi.org/10.1016/S0165-9936\(03\)00603-4](https://doi.org/10.1016/S0165-9936(03)00603-4)
- Fakhri A, Adami S (2014) Adsorption and thermodynamic study of Cephalosporins antibiotics from aqueous solution onto MgO nanoparticles. *J Taiwan Inst Chem Eng* 45:1001–1006. <https://doi.org/10.1016/j.jtice.2013.09.028>
- Fang Z, Chen J, Qiu X, Qiu X, Cheng W, Zhu L (2011) Effective removal of antibiotic metronidazole from water by nanoscale zero-valent iron particles. *Desalination* 268:60–67. <https://doi.org/10.1016/j.desal.2010.09.051>
- Golcu A, Dogan B, Ozkan SA (2005) Anodic voltammetric behavior and determination of cefixime in pharmaceutical dosage forms and biological fluids. *Talanta* 67:703–712. <https://doi.org/10.1016/j.talanta.2005.03.020>
- Gonçalves MST, Oliveira-Campos AMF, Pinto EMMS., Plasência PMS, Queiroz MJRP. (1999) Photochemical treatment of solutions of azo dyes containing TiO. *Chemosphere* 39 2:781–786. [https://doi.org/10.1016/S0045-6535\(99\)00013-2](https://doi.org/10.1016/S0045-6535(99)00013-2)
- Grčić I, Papić S, Žižek K, Koprivanac N (2012) Zero-valent iron (ZVI) Fenton oxidation of reactive dye wastewater under UV-C and solar irradiation. *Chem Eng J* 195–196:77–90. <https://doi.org/10.1016/j.cej.2012.04.093>
- Guo R, Chen J (2015) Application of alga-activated sludge combined system (AASCS) as a novel treatment to remove cephalosporins. *Chem Eng J* 260:550–556. <https://doi.org/10.1016/j.cej.2014.09.053>
- Gupta VK, Nayak A (2012) Cadmium removal and recovery from aqueous solutions by novel adsorbents prepared from orange peel and Fe<sub>2</sub>O<sub>3</sub> nanoparticles. *Chem Eng J* 180:81–90. <https://doi.org/10.1016/j.cej.2011.11.006>
- Gupta VK, Mittal A, Gajbe V (2005) Adsorption and desorption studies of a water soluble dye, Quinoline Yellow, using waste materials. *J Colloid Interface Sci* 284:89–98. <https://doi.org/10.1016/j.jcis.2004.09.055>
- Gupta VK, Carrott PJM, Ribeiro Carrott MML, Suhas (2009) Low-cost adsorbents: growing approach to wastewater treatment—a Review. *Crit Rev Environ Sci Technol* 39:783–842. <https://doi.org/10.1080/10643380801977610>
- Gupta VK, Jain R, Nayak A, Agarwal S, Shrivastava M (2011) Removal of the hazardous dye—tartrazine by photodegradation

- on titanium dioxide surface. *Mater Sci Eng C* 31:1062–1067. <https://doi.org/10.1016/j.msec.2011.03.006>
- Gupta VK, Jain R, Mittal A, Saleh TA, Nayak A, Agarwal S, Sikarwar S (2012) Photo-catalytic degradation of toxic dye amaranth on TiO<sub>2</sub>/UV in aqueous suspensions. *Mater Sci Eng C* 32:12–17. <https://doi.org/10.1016/j.msec.2011.08.018>
- Gupta VK, Kumar R, Nayak A, Saleh TA, Barakat MA (2013) Adsorptive removal of dyes from aqueous solution onto carbon nanotubes: a review. *Adv Colloid Interface Sci* 193–194:24–34 <https://doi.org/10.1016/j.cis.2013.03.003>
- Herrmann JM, Guillard C, Pichat P (1993) Heterogeneous photocatalysis: an emerging technology for water treatment. *Catal Today* 17:7–20. [https://doi.org/10.1016/0920-5861\(93\)80003-J](https://doi.org/10.1016/0920-5861(93)80003-J)
- Hirsch R, Ternes T, Haberer K, Kratz K-L (1999) Occurrence of antibiotics in the aquatic environment. *Sci Total Environ* 225:109–118. [https://doi.org/10.1016/S0048-9697\(98\)00337-4](https://doi.org/10.1016/S0048-9697(98)00337-4)
- Hoffmann I, Oppel C, Gernert U, Barreleiro P, von Rybinski W, Gradzielski M (2012) Adsorption isotherms of cellulose-based polymers onto cotton fibers determined by means of a direct method of fluorescence. *Spectrosc Langmuir* 28:7695–7703. <https://doi.org/10.1021/la300192q>
- Huang Y, Yamaguchi A, Pham TD, Kobayashi M (2017) Charging and aggregation behavior of silica particles in the presence of lysozymes. *Colloid Polym Sci*. <https://doi.org/10.1007/s00396-017-4226-2>
- Jain R, Gupta VK, Jadon N, Radhapyari K (2010) Voltammetric determination of cefixime in pharmaceuticals and biological fluids. *Anal Biochem* 407:79–88. <https://doi.org/10.1016/j.ab.2010.07.027>
- Joseph LK, Dayas KR, Damodar S, Krishnan B, Krishnankutty K, Nampoori VPN, Radhakrishnan P (2008) Photoluminescence studies on rare earth titanates prepared by self-propagating high temperature synthesis method. *Spectrochim Acta A* 71:1281–1285. <https://doi.org/10.1016/j.saa.2008.03.030>
- Kandhro AA, Laghari AH, Mahesar SA, Saleem R, Nelofar A, Khan ST, Sherazi STH (2013) Application of attenuated total reflectance Fourier transform infrared spectroscopy for determination of cefixime in oral pharmaceutical formulations. *Spectrochim Acta A* 115:51–56. <https://doi.org/10.1016/j.saa.2013.06.032>
- Karthikeyan S, Gupta VK, Boopathy R, Titus A, Sekaran G (2012) A new approach for the degradation of high concentration of aromatic amine by heterocatalytic Fenton oxidation: Kinetic and spectroscopic studies. *J Mol Liq* 173:153–163. <https://doi.org/10.1016/j.molliq.2012.06.022>
- Khataee AR, Kasiri MB (2010) Photocatalytic degradation of organic dyes in the presence of nanostructured titanium dioxide: Influence of the chemical structure of dyes. *J Mol Catal A* 328:8–26. <https://doi.org/10.1016/j.molcata.2010.05.023>
- Kitamura S, Koda S, Miyamae A, Yasuda T, Morimoto Y (1990) Dehydration effect on the stability of cefixime trihydrate. *Int J Pharm* 59:217–224. [https://doi.org/10.1016/0378-5173\(90\)90112-H](https://doi.org/10.1016/0378-5173(90)90112-H)
- Klauson D, Babkina J, Stepanova K, Krichevskaya M, Preis S (2010) Aqueous photocatalytic oxidation of amoxicillin. *Catal Today* 151:39–45. <https://doi.org/10.1016/j.cattod.2010.01.015>
- Kobayashi M (2008) Electrophoretic mobility of latex spheres in the presence of divalent ions: experiments and modeling. *Colloid Polym Sci* 286:935–940. <https://doi.org/10.1007/s00396-008-1851-9>
- Kümmerer K (2009) Antibiotics in the aquatic environment—a review—part II. *Chemosphere* 75:435–441. <https://doi.org/10.1016/j.chemosphere.2008.12.006>
- Le Corre KS, Ort C, Kateley D, Allen B, Escher BI, Keller J (2012) Consumption-based approach for assessing the contribution of hospitals towards the load of pharmaceutical residues in municipal wastewater. *Environ Int* 45:99–111. <https://doi.org/10.1016/j.envint.2012.03.008>
- Magit AE, Dolitsky JN, Doyle WJ, Swarts JD, Seroky JT, Rosenfeld RM (1994) An experimental study of cefixime in the treatment of *Streptococcus pneumoniae* otitis media. *Int J Pediatr Otorhinolaryngol* 29:1–9. [https://doi.org/10.1016/0165-5876\(94\)90103-1](https://doi.org/10.1016/0165-5876(94)90103-1)
- Mallick S, Mondal A, Sannigrahi S (2008) Kinetic measurements of the hydrolytic degradation of cefixime: effect of Captisol complexation and water-soluble polymers. *J Pharm Pharmacol* 60:833–841. <https://doi.org/10.1211/jpp.60.7.0004>
- Michael I et al (2013) Urban wastewater treatment plants as hotspots for the release of antibiotics in the environment: a review. *Water Res* 47:957–995. <https://doi.org/10.1016/j.watres.2012.11.027>
- Midtvedt T (2008) 25-Penicillins, cephalosporins, other beta-lactam antibiotics, and tetracyclines. In: Aronson JK (ed) *Side effects of drugs annual*, vol 30. Elsevier, pp 280–296
- Mittal A, Kaur D, Malviya A, Mittal J, Gupta VK (2009) Adsorption studies on the removal of coloring agent phenol red from wastewater using waste materials as adsorbents. *J Colloid Interface Sci* 337:345–354. <https://doi.org/10.1016/j.jcis.2009.05.016>
- Patterson AL (1939) The Scherrer formula for X-ray particle size determination. *Phys Rev* 56:978–982
- Pham TD, Kobayashi M, Adachi Y (2014) Adsorption of polyanion onto large alpha alumina beads with variably charged surface. *Adv Phys Chem* 2014:9. <https://doi.org/10.1155/2014/460942>
- Pham TD, Kobayashi M, Adachi Y (2015a) Adsorption characteristics of anionic azo dye onto large  $\alpha$ -alumina beads. *Colloid Polym Sci* 293:1877–1886. <https://doi.org/10.1007/s00396-015-3576-x>
- Pham TD, Kobayashi M, Adachi Y (2015b) Adsorption of anionic surfactant sodium dodecyl sulfate onto alpha alumina with small surface area. *Colloid Polym Sci* 293:217–227. <https://doi.org/10.1007/s00396-014-3409-3>
- Pham TD et al (2017a) Adsorptive removal of ammonium ion from aqueous solution using surfactant-modified alumina. *Environ Chem* 14:327–337. <https://doi.org/10.1071/EN17102>
- Pham TD et al (2017b) Adsorptive removal of copper by using surfactant modified laterite soil. *J Chem* 2017:10. <https://doi.org/10.1155/2017/1986071>
- Pham TD et al (2018) Adsorption of polyelectrolyte onto nanosilica synthesized from rice husk: characteristics, mechanisms, and application for antibiotic removal. *Polymers* 10:220
- Pourtaheri A, Nezamzadeh-Ejehieh A (2015) Photocatalytic properties of incorporated NiO onto clinoptilolite nano-particles in the photodegradation process of aqueous solution of cefixime pharmaceutical capsule. *Chem Eng Res Des* 104:835–843. <https://doi.org/10.1016/j.cherd.2015.10.031>
- Praveena R, Shi L, Jang KH, Venkatramu V, Jayasankar CK, Seo HJ (2011) Sol–gel synthesis and thermal stability of luminescence of Lu<sub>3</sub>Al<sub>5</sub>O<sub>12</sub>:Ce<sup>3+</sup> nano-garnet. *J Alloy Compd* 509:859–863. <https://doi.org/10.1016/j.jallcom.2010.09.113>
- Prida VM et al (2007) Temperature influence on the anodic growth of self-aligned titanium dioxide nanotube arrays. *J Magn Magn Mater* 316:110–113. <https://doi.org/10.1016/j.jmmm.2007.02.021>
- Saleh TA, Gupta VK (2014) Processing methods, characteristics and adsorption behavior of tire derived carbons: a review. *Adv Colloid Interface Sci* 211:93–101. <https://doi.org/10.1016/j.cis.2014.06.006>
- Santiago-Morales J, Gómez MJ, Herrera-López S, Fernández-Alba AR, García-Calvo E, Rosal R (2013) Energy efficiency for the removal of non-polar pollutants during ultraviolet irradiation, visible light photocatalysis and ozonation of a wastewater effluent. *Water Res* 47:5546–5556. <https://doi.org/10.1016/j.watres.2013.06.030>
- Saravanan R, Gupta VK, Narayanan V, Stephen A (2013a) Comparative study on photocatalytic activity of ZnO prepared by different methods. *J Mol Liq* 181:133–141. <https://doi.org/10.1016/j.molliq.2013.02.023>

- Saravanan R, Karthikeyan N, Gupta VK, Thirumal E, Thangadurai P, Narayanan V, Stephen A (2013b) ZnO/Ag nanocomposite: an efficient catalyst for degradation studies of textile effluents under visible light. *Mater Sci Eng C* 33:2235–2244 <https://doi.org/10.1016/j.msec.2013.01.046>
- Saravanan R, Karthikeyan S, Gupta VK, Sekaran G, Narayanan V, Stephen A (2013c) Enhanced photocatalytic activity of ZnO/CuO nanocomposite for the degradation of textile dye on visible light illumination. *Mater Sci Eng C* 33:91–98. <https://doi.org/10.1016/j.msec.2012.08.011>
- Saravanan R, Thirumal E, Gupta VK, Narayanan V, Stephen A (2013d) The photocatalytic activity of ZnO prepared by simple thermal decomposition method at various temperatures. *J Mol Liq* 177:394–401. <https://doi.org/10.1016/j.molliq.2012.10.018>
- Saravanan R, Gracia F, Khan MM, Poornima V, Gupta VK, Narayanan V, Stephen A (2015a) ZnO/CdO nanocomposites for textile effluent degradation and electrochemical detection. *J Mol Liq* 209:374–380. <https://doi.org/10.1016/j.molliq.2015.05.040>
- Saravanan R, Mansoob Khan M, Gupta VK, Mosquera E, Gracia F, Narayanan V, Stephen A (2015b) ZnO/Ag/CdO nanocomposite for visible light-induced photocatalytic degradation of industrial textile effluents. *J Colloid Interface Sci* 452:126–133. <https://doi.org/10.1016/j.jcis.2015.04.035>
- Saravanan R, Sacari E, Gracia F, Khan MM, Mosquera E, Gupta VK (2016) Conducting PANI stimulated ZnO system for visible light photocatalytic degradation of coloured dyes. *J Mol Liq* 221:1029–1033. <https://doi.org/10.1016/j.molliq.2016.06.074>
- Schwartz T, Kohnen W, Jansen B, Obst U (2003) Detection of antibiotic-resistant bacteria and their resistance genes in wastewater, surface water, and drinking water biofilms. *FEMS Microbiol Ecol* 43:325–335. <https://doi.org/10.1111/j.1574-6941.2003.tb01073.x>
- Shojaie AF, Loghmani MH (2010) La<sup>3+</sup> and Zr<sup>4+</sup> co-doped anatase nano TiO<sub>2</sub> by sol-microwave method. *Chem Eng J* 157:263–269. <https://doi.org/10.1016/j.cej.2009.12.025>
- Song Y, Tian Q, Zou R, Chen Z, Yang J, Hu J (2011) Phase and luminescent intensity control of hydrophilic rare-earth up-converting nanophosphors prepared by one-pot solvothermal synthesis. *J Alloy Compd* 509:6539–6544. <https://doi.org/10.1016/j.jallcom.2011.03.122>
- Sousa VM, Manaia CM, Mendes A, Nunes OC (2013) Photoinactivation of various antibiotic resistant strains of *Escherichia coli* using a paint coat. *J Photochem Photobiol A* 251:148–153. <https://doi.org/10.1016/j.jphotochem.2012.10.027>
- Wu Y, Hu X, Xie T, Li G, Zhang L (2005) Phase structure of W-doped nano-TiO<sub>2</sub> produced by sol-gel method. *China Particuol* 3:233–236. [https://doi.org/10.1016/S1672-2515\(07\)60193-6](https://doi.org/10.1016/S1672-2515(07)60193-6)
- Yamaguchi A, Kobayashi M (2016) Quantitative evaluation of shift of slipping plane and counterion binding to lysozyme by electrophoresis method. *Colloid Polym Sci* 294:1019–1026. <https://doi.org/10.1007/s00396-016-3852-4>
- Zare K, Sadegh H, Shahryari-ghoshekandi R, Asif M, Tyagi I, Agarwal S, Gupta VK (2016) Equilibrium and kinetic study of ammonium ion adsorption by Fe<sub>3</sub>O<sub>4</sub> nanoparticles from aqueous solutions. *J Mol Liq* 213:345–350. <https://doi.org/10.1016/j.molliq.2015.08.045>